nature geoscience

ARTICLES

https://doi.org/10.1038/s41561-020-0550-0

Distinct oxygen isotope compositions of the Earth and Moon

Erick J. Cano[1]✉, Zachary D. Sharp[1] and Charles K. Shearer[2]

The virtually identical oxygen isotope compositions of the Earth and Moon revealed by Apollo return samples have been a challenging constraint for lunar formation models. For a giant impact scenario to explain this observation, either the precursors to the Earth and Moon had identical oxygen isotope values or extensive homogenization of the two bodies occurred following the impact event. Here we present high-precision oxygen isotope analyses of a range of lunar lithologies and show that the Earth and Moon in fact have distinctly different oxygen isotope compositions. Oxygen isotope values of lunar samples correlate with lithology, and we propose that the differences can be explained by mixing between isotopically light vapour, generated by the impact, and the outermost portion of the early lunar magma ocean. Our data suggest that samples derived from the deep lunar mantle, which are isotopically heavy compared to Earth, have isotopic compositions that are most representative of the proto-lunar impactor 'Theia'. Our findings imply that the distinct oxygen isotope compositions of Theia and Earth were not completely homogenized by the Moon-forming impact, thus providing quantitative evidence that Theia could have formed farther from the Sun than did Earth.

Earth's Moon is thought to have formed from the debris of a large-scale collision between a partially formed proto-Earth and a smaller proto-planet given the informal name 'Theia'[1–5]. The giant-impact hypothesis, first proposed by two independent and contemporaneous studies[1,2], is the currently favoured explanation for the Moon's origin. This model was capable of accounting for the then-recent observations from samples returned by the Apollo missions, which included the Moon's low iron content relative to Earth, depletion in volatiles and enrichment in refractory elements, while avoiding most of the pitfalls of previous lunar origin theories. Early numerical simulations of planetary collisions generally supported the giant impact[3,6–9], finding that a single large impact could (1) produce the initial angular momentum of the Earth–Moon system and (2) eject a sufficient amount of iron-depleted material into orbit to form the Moon. However, models of the classic style of giant impact predicted that the Moon would have accreted from approximately 70–90% of the proto-lunar impactor Theia[5].

Having such a large portion of the Moon originate from Theia has proven to be a major issue for the giant-impact hypothesis because it has been observed that the Earth and Moon have nearly identical non-volatile isotope ratios[10–13]. Looking specifically at the triple oxygen isotope system, analyses of lunar basalt samples have produced average $\Delta'^{17}O$ values ($\Delta'^{17}O = \delta'^{17}O - \lambda\delta'^{18}O$, see Methods) that are virtually indistinguishable from Earth's[14–17]. This compositional conundrum of nearly identical oxygen isotope compositions for the Earth and Moon has led to numerous models that have sought to explain these similarities in the context of the giant impact. The simplest explanation is that proto-Earth and Theia initially had nearly identical $\Delta'^{17}O$ values, implying that the proto-Earth and Theia must have formed at similar heliocentric distances from the same isotopic reservoir[14,18]. Alternatively, isotopic re-equilibration occurred between the Earth and Moon immediately after the giant impact such that any original isotopic heterogeneities were erased. This could have occurred through isotopic exchange within a vapour component[19–21] or as the product of a larger, more energetic collision[22–24].

The extreme similarity for the $\Delta'^{17}O$ values of the Earth and Moon has been seen in a number of recent high-precision oxygen isotope studies. Herwartz et al.[25] suggest that the Moon has a slightly higher $\Delta'^{17}O$ value than the Earth by 12 ± 3 ppm (0.012‰). Young et al.[17] and Greenwood et al.[26] suggest that the differences are only -1 ± 5 ppm (−0.001‰) and 4 ± 3 ppm (0.004‰), respectively. We expand on the previous work by performing high-precision, whole-rock and mineral separate oxygen isotope analyses on a wide variety of lunar lithologies. We show that the method of averaging together lunar isotope data while ignoring lithological differences does not give an accurate picture of the differences between the Earth and Moon.

Isotopic variations among lunar lithologies

Here we show that, when considered in terms of lithology and mineral separate data, there are distinct differences in the $\Delta'^{17}O$ values of different lunar lithologies. We propose that these varying $\Delta'^{17}O$ values are due to differing degrees of incorporation of an isotopically light silicate atmosphere that formed as a result of the giant impact. The least-contaminated materials, those of deep origin, have $\Delta'^{17}O$ values that are statistically distinct from Earth.

Oxygen isotope analyses were performed at the Center for Stable Isotopes at the University of New Mexico using the standard laser fluorination technique[27] modified to obtain high-precision $\Delta'^{17}O$ measurements (see Methods). Our analytical precision, based on the repeated analysis of a San Carlos olivine internal standard (Supplementary Table 1), is ±0.138‰ for $\delta^{18}O$ and ±0.004‰ for $\Delta'^{17}O$ ($n = 44$, 1σ s.d.). We measured bulk and mineral separates from a suite of lunar samples that included high- and low-Ti mare basalts, highland anorthosites, norites and volcanic glasses. A suite of terrestrial mantle-derived samples was also measured to determine the $\Delta'^{17}O$ value of the bulk silicate Earth (BSE) (Supplementary Table 2).

[1]Department of Earth and Planetary Sciences, University of New Mexico, Albuquerque, NM, USA. [2]Institute of Meteoritics, University of New Mexico, Albuquerque, NM, USA. ✉e-mail: ejcano@unm.edu

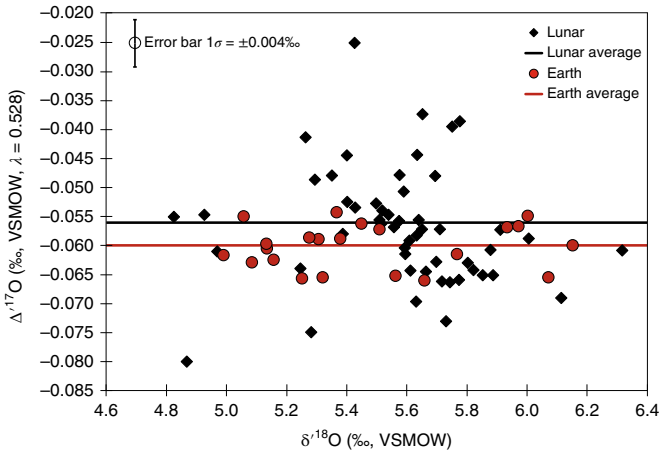

Fig. 1 | Plot of $\Delta'^{17}O$ versus $\delta'^{18}O$ for lunar and terrestrial samples. Lunar samples are represented by the black diamonds, and terrestrial samples are represented by the red circles. Lunar samples include both whole-rock and mineral separate data. A combination of whole-rock and mafic mineral separates, which were used for the BSE calculation, are plotted for the terrestrial samples. The error bar represents 1σ s.d. The black line and red line indicate the mean values for the lunar samples and terrestrial samples, respectively. The lunar samples display a much larger range of $\Delta'^{17}O$ variability with a s.d. of 0.0103‰ (1σ), about three times that of the Earth's 0.0037‰ (1σ) s.d.

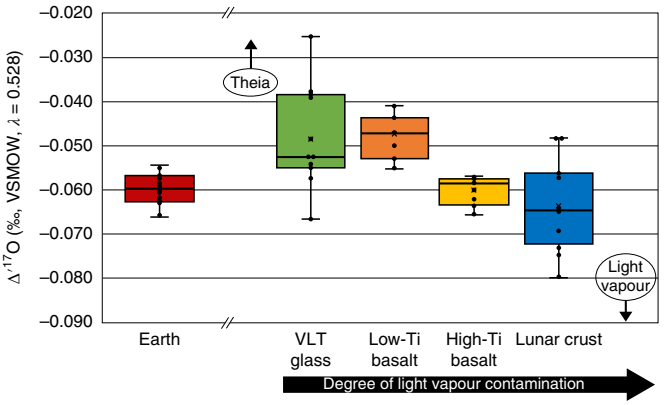

Fig. 2 | Box-and-whisker plot showing the $\Delta'^{17}O$ values for the different lunar lithologies and Earth. The $\Delta'^{17}O$ values decrease with increasing degree of contamination from the light vapour. All data points are plotted as black circles. The bar in each box is the median value, and the X denotes the mean value. The upper and lower quartiles are defined by the upper and lower borders of the coloured box, respectively, and the whiskers represent the upper and lower extremes of the data. Note that the high-Ti basalts occupy nearly the same $\Delta'^{17}O$ range as the BSE. The spacing on the *x* axis between the different groups is not quantitative; however, the order proceeds from left to right with increasing degrees of contamination. Whole-rock values were primarily used for the low- and high-Ti basalt data on this plot; however, it was necessary to supplement 'lunar crust' data with mineral separate data.

Averaging the $\Delta'^{17}O$ values obtained from our measurements of bulk lunar samples to determine the value for the bulk silicate Moon, as was done in previous studies (for example,[14–17,25,26]), yields a $\Delta'^{17}O$ value of -0.056 ± 0.010‰ (1σ s.d. $n = 23$) (Fig. 1). This is practically indistinguishable from the BSE value of -0.060 ± 0.004‰ (1σ s.d. $n = 22$). However, it is more noteworthy that lunar samples have nearly three times the $\Delta'^{17}O$ variability (1$\sigma = 0.0103$‰) when compared with Earth (1$\sigma = 0.0037$‰).

When considered in terms of lithology, distinct $\Delta'^{17}O$ differences are seen between different rock types (Fig. 2). We propose that the variation seen in the lunar $\Delta'^{17}O$ values is caused by the mixing of two distinct isotopic reservoirs. The first is the deep lunar mantle material, which most-closely retains the original $\Delta'^{17}O$ value of the proto-lunar impactor, and the second is a low $\Delta'^{17}O$ component formed from the incorporation of an isotopically light condensed silicate vapour atmosphere produced during the giant impact. The bulk Moon values are most closely represented by the low-Ti basalts and some deeply sourced very low-Ti (VLT) glass, which contain a minimal fraction of the light vapour. Samples that received a larger fraction of the light vapour, such as the high-Ti basalts, high-Ti glass, KREEPy (rich in potassium (K), rare-earth elements (REE) and phosphorus (P)) lithologies and ferroan anorthosites (FANs), have statistically significant lower $\Delta'^{17}O$ values.

The mare basalts show a relationship of decreasing $\Delta'^{17}O$ values with increasing TiO_2 content (Fig. 3). The low-Ti basalts range between -0.044‰ and -0.055‰ with an average of -0.050‰. Two pyroxene separates from the low-Ti basalts, which are more resistant to isotopic exchange than plagioclase or glass (see Supplementary Information), have $\Delta'^{17}O$ values of -0.041‰ and -0.044‰. These high $\Delta'^{17}O$ values are 4–5 sigma outliers from the terrestrial mantle range. By contrast, the high-Ti basalts range between -0.057‰ and -0.064‰ and have an average of -0.060‰, which is coincidentally indistinguishable from the values of BSE (Fig. 3). Comparing the bulk and mineral separate data of the low- and high-Ti basalts (excluding plagioclase due to its susceptibility to alteration, see Supplementary Information) yields a two-tailed *P* value of 0.0003, which, by conventional criteria, is considered to be 'extremely statistically significant'. This trend is also seen to some extent in the lunar volcanic glasses, which are thought to represent near-primary magmas[28,29]. Certain fractions of the Apollo 15 VLT green glass (15426) have $\Delta'^{17}O$ values as high as -0.025‰ while others are as low as -0.066‰ (Fig. 3, this range is discussed in the following). By contrast, the $\Delta'^{17}O$ value of -0.056‰ for the Apollo 17 high-Ti orange/black glass (74220) is statistically indistinguishable from similarly high-Ti basalts (Fig. 3). It could be argued that the high $\Delta'^{17}O$ value of the green glass is a result of modification during eruption; however, no high-temperature process is known to increase the $\Delta'^{17}O$ value. If such a process existed, we would then expect to see universally high $\Delta'^{17}O$ values for all the glasses; however, the high-Ti orange/black glass is virtually identical to the high-Ti basalts and shows minimal variation.

The spread of $\Delta'^{17}O$ values measured in the various fractions of the VLT green glass covers a range over three times that of high-Ti glass or mid-ocean-ridge basalt (MORB) glass measurements and does not appear to be an analytical artifact (Extended Data Fig. 4 and Supplementary Information). These values are explained through mixing between a heavy bulk Moon value and light material previously contaminated by the light silicate vapour atmosphere (Extended Data Fig. 5 and Supplementary Information). Numerous studies support the view that the VLT green glasses were derived from early lunar magma ocean (LMO) cumulate sources below depths of 400 km and have not experienced extensive fractional crystallization like many of the sampled crystalline mare basalts[28–30]. We therefore assume that the heaviest $\Delta'^{17}O$ values exhibited by the VLT green glass are representative of near-primary melts derived from deep within the lunar mantle. These melts should presumably have the lowest amount of light vapour contamination and heaviest $\Delta'^{17}O$ values. The VLT green glass fractions with the highest $\Delta'^{17}O$ values are interpreted as the heavy endmember to which lighter material was added, producing the variation. Even ignoring the singular highest VLT green glass value (-0.025‰) as a possible

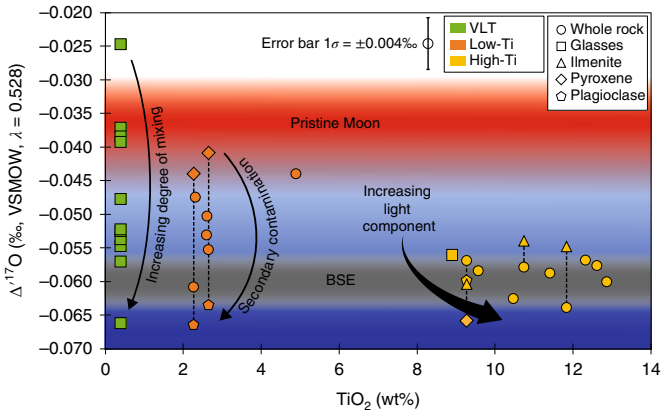

Fig. 3 | Plot of $\Delta'^{17}O$ versus TiO_2 content for high- and low-Ti lunar mare basalts, volcanic glasses and associated mineral separates. The TiO_2 values used for this plot are averaged from the major oxide data found in the Lunar Sample Compendium[43] and the references found therein. Whole-rock samples are linked to their corresponding mineral separates by dashed lines. The heaviest VLT glass probably represents the pristine lunar mantle with several pyroxene separates approaching this value (red band). Increasing incorporation of light-vapour-contaminated material lowers the $\Delta'^{17}O$ values, as seen in the high-Ti basalts and easily exchangeable plagioclase separates from two low-Ti basalts, bringing them closer to the range of the Earth's mantle (grey band).

outlier, the next-highest cluster of $\Delta'^{17}O$ values occurs at an average of −0.038‰. This high value is nearly matched by the two refractory pyroxene separates from low-Ti basalts and is assumed to be a minimum estimate for the uncontaminated Theia component, with the possibility for heavier values to exist.

Isotopic fractionation during vapour condensation and melt crystallization

A silicate vapour envelope is thought to have formed around a molten Moon after the giant impact[19,31]. Experiments have shown that there is a large ^{17}O mass independent fractionation during condensation of SiO_2 from SiO gas in the presence of hydrogen[32]. The condensing SiO_2 is enriched in ^{17}O while the residual vapour can attain significantly lower $\Delta'^{17}O$ values through simple Rayleigh fractionation (Extended Data Fig. 1 and Supplementary Information). The early-formed condensate from the silicate vapour would be well mixed back into the LMO before any stratification occurred, such that it would not produce a measurable effect on the overall oxygen isotope composition of the lunar mantle. The residual low $\Delta'^{17}O$ vapour would be incorporated into the outermost portion of the LMO once stratification began to occur. On the basis of dynamic models for LMO convection[33], this light signature contaminated material could remain sequestered in the viscous surface layer of a stratified magma ocean, unmixed into the deeper portions of the LMO. The low $\Delta'^{17}O$ values of troctolitic anorthosites and regolith breccias are explained by the incorporation of this surface-layer contamination.

The early-formed crustal samples, including ferroan anorthosites and emplaced Mg-suite rocks, generally have the lowest $\Delta'^{17}O$ values, implying that they have the largest degree of light vapour incorporation, consistent with their respective formation processes[34,35]. The other endmember is a deeply sourced mantle cumulate that would presumably have the lowest amount of light vapour contamination and the highest $\Delta'^{17}O$ values. Logically, the deeply sourced VLT green glass (sample 15426) fractions with the highest $\Delta'^{17}O$ values seen in this study should be representative of this uncontaminated mantle source. These high values are our minimum estimate for the non-contaminated Theia component that is preserved in the early-formed olivine + pyroxene mantle cumulates. It could be argued that the isotopically heavy value of the green glass is a product of the early-formed ^{17}O-enriched SiO_2 condensate produced as a complement to the light vapour. However, this initial material that rained out would have been remixed into the deeper convective portion of the LMO. On the basis of the great depths at which the parent magmas for these glasses are formed[28] and the small proportion of heavy condensate relative to the greater LMO, preservation of these isotopically heavy values in deeply sourced samples is inconsistent with convection models for the deeper regions of the LMO[33]. Simple mass balance argues against any measurable isotope shift.

The isotopic differences between the low- and high-Ti basalts are also explained in terms of conventional lunar crystallization models. Crystallization of the LMO produced cumulates with a large variety of compositions that are thought to be sources for the later periods of lunar basaltic magmatism[36]. Formation of the high- and low-Ti mare basalts involved the mixing of at least two lunar reservoirs with different oxygen isotope compositions. One of these reservoirs was the deeply sourced, early-formed lunar mantle cumulates that most closely preserved the values of Theia. The other was derived in part from the late-stage LMO cumulates that crystallized in regions where the light vapour contamination occurred. The initial crystallization of the LMO produced olivine and pyroxene cumulates that settled towards the base of the LMO preserving the proto-lunar impactor $\Delta'^{17}O$ signature. The Ti-rich pyroxene + ilmenite ± olivine cumulates, which formed in the last stages of LMO crystallization (>90% crystallization), would have been produced from materials that experienced light vapour contamination, similar to the FANs. These ilmenite-bearing cumulates (IBCs) with low $\Delta'^{17}O$ values were gravitationally unstable in relation to their surrounding materials due to their high density[37,38]. The IBCs, having formed near the top of the cumulate pile, forced the mantle to undergo overturn to reach a gravitationally stable state. Through the overturn process, the IBCs sank into the underlying olivine + pyroxene cumulates, where they mixed, initiating partial melting[39,40]. Magmas formed from the partial melting of these cumulates, which were hybridized to varying degrees, are thought to be the source for the high-Ti mare basalts and possibly the entire spectrum of mare basalts[28,37–40]. It is therefore reasonable to propose that these hybrid magmas could be responsible for both the range of TiO_2 compositions in mare basalts and the variation in $\Delta'^{17}O$ values. Hybrid magmas that contained a larger percentage of IBCs were imbued with higher TiO_2 compositions. The high-Ti basalts that evolved from these magmas have $\Delta'^{17}O$ values lower than those of the less-contaminated low-Ti basalts and average to around the same $\Delta'^{17}O$ value as the BSE. The low-Ti basalts evolved from magmas that contained a smaller contribution from IBCs and, therefore, retained an isotopic signature closer to that of the deep olivine and pyroxene cumulates.

Some low-Ti basalts have undergone a secondary interaction with isotopically light material. The low $\Delta'^{17}O$ values of some plagioclase separates indicate contamination by a light near-surface component during passage through the crust, whereas the more refractory pyroxene separates retain the deep-sourced mantle $\Delta'^{17}O$ value. In whole-rock samples, this secondary contamination of the plagioclase draws down their overall $\Delta'^{17}O$ values from that preserved by the pyroxenes. This secondary effect is not seen as drastically in the high-Ti basalts either due to a lack of assimilation of the low $\Delta'^{17}O$ component during ascent or because the high-Ti basalts' magmatic source already had lower $\Delta'^{17}O$ values due to a higher degree of contamination from the IBCs, subduing or masking the effect.

A similar effect is likely responsible for the non-equilibrium values observed in the mineral separates from a lunar troctolite

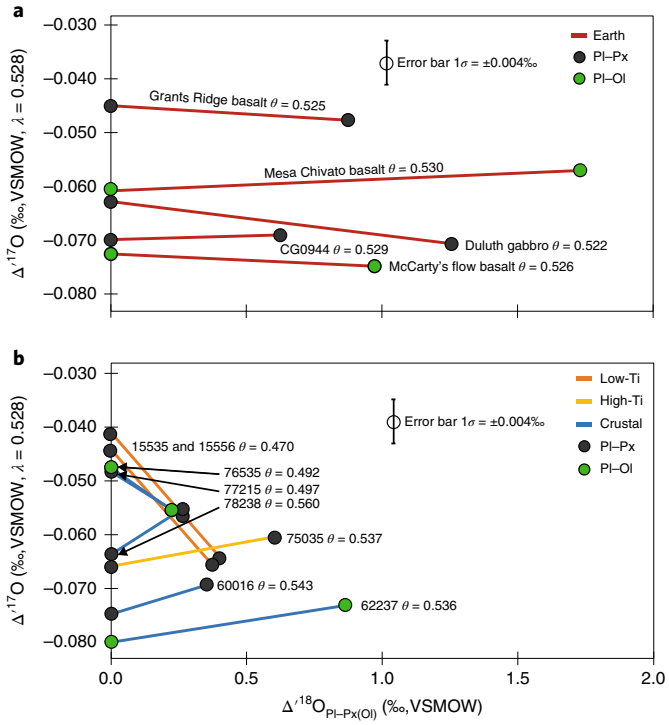

Fig. 4 | Plot of $\Delta'^{17}O$ versus $\Delta'^{18}O_{Pl-Px/Ol}$ and θ values for mineral pairs of terrestrial and lunar samples. The θ values are defined by the slope of the line connecting the mineral pair and are labelled next to the sample name. All pyroxene or olivine separate data are plotted at the *y* axis where $\Delta'^{18}O_{Pl-Px/Ol}$ is equal to zero. **a**, The mineral separate data are plotted for the terrestrial samples. All pairs have θ values of 0.522 to 0.530. **b**, Mineral separate data are plotted for the lunar samples, including two low-Ti basalts, a high-Ti basalt and crustal rocks, including one FAN sample (62237). The θ values for lunar samples cover a wide range from 0.470 to 0.560, clearly demonstrating disequilibrium due to the mixing of two reservoirs with distinct $\Delta'^{17}O$ values (see Supplementary Information).

(76535) and a cataclastic norite (77215). These Mg suite plutonic rocks brought from depth during LMO cumulate overturn are thought to have assimilated KREEP and FAN material at the base of the crust prior to emplacement[35]. As late-stage products of LMO crystallization, KREEP and FAN material would incorporate material contaminated by the light vapour component, producing an effect similar to that seen in the mare basalts, decreasing their $\Delta'^{17}O$ values. The varying effect of this mixing is demonstrated by the wide range of $\Delta'^{17}O$ values exhibited by the lunar 'crustal' suite compared with the low-Ti basalts and terrestrial mantle samples (Fig. 2).

Further evidence for two-component mixing is seen in the mineral separate data. Triple oxygen isotope equilibrium can be assessed from the θ values, where $\theta_{A-B} = \left(\delta'^{17}O_A - \delta'^{17}O_B\right)/\left(\delta'^{18}O_A - \delta'^{18}O_B\right)$. At high temperatures, θ should be in the range of 0.528 to 0.530[41,42]. Coexisting pyroxene–plagioclase pairs from terrestrial basalts range from 0.522 to 0.530 (±0.004, 1σ) (Fig. 4a). By contrast, lunar samples have extremely varied θ values from 0.470 to 0.560, providing clear evidence of disequilibrium (Fig. 4b). Pyroxene from low-Ti basalts 15535 and 15556 have $\Delta'^{17}O$ values close to the presumed pristine lunar mantle (−0.044‰ and −0.041‰), whereas coexisting plagioclase has low $\Delta'^{17}O$ values of −0.066‰ and −0.064‰, explained by secondary contamination by light crustal material to the more easily exchangeable plagioclase during passage of the magmas through the crust (Fig. 3). Incorporation of the light vapour should raise the $\delta^{18}O$ value of the most affected samples by ~0.6‰, which is consistent with the $\delta^{18}O$ shifts observed (Extended Data Fig. 2 and Supplementary Information).

There is a trend of decreasing $\Delta'^{17}O$ values with an increasing degree of contamination ranging from the least-contaminated VLT green glass through the lunar crustal material (Fig. 2). The proto-lunar impactor Theia, therefore, probably had a $\Delta'^{17}O$ value of −0.038‰ or greater to produce the range of values seen in lunar samples. The original $\Delta'^{17}O$ value of Theia is a function of the degree of mixing following the giant impact. If we assume that the Moon is composed of 70–90% Theia, then the initial $\Delta'^{17}O$ of the Theia precursor is −0.028‰ to −0.035‰ (Extended Data Fig. 3 and Supplementary Information). If the oxygen isotope heterogeneity of terrestrial bodies in the inner solar system trends towards higher $\Delta'^{17}O$ values with heliocentric distance, Theia would have an origin farther out from the Sun relative to Earth. Clearly, Theia's distinct oxygen isotope composition was not completely lost through homogenization during the giant impact. This result thereby eliminates the necessity for giant-impact models to include a mechanism for complete oxygen isotope homogenization between the two bodies and provides a foundation for future modelling of the impact and lunar formation.

Online content

Any methods, additional references, Nature Research reporting summaries, source data, extended data, supplementary information, acknowledgements, peer review information; details of author contributions and competing interests; and statements of data and code availability are available at https://doi.org/10.1038/s41561-020-0550-0.

Received: 23 October 2019; Accepted: 3 February 2020;
Published online: 09 March 2020

References

1. Hartmann, W. K. & Davis, D. R. Satellite-sized planetesimals and lunar origin. *Icarus* **24**, 504–515 (1975).
2. Cameron, A. G. W. & Ward, W. R. The origin of the Moon. *Abstr. Lunar Planet. Sci. Conf.* **7**, 120 (1976).
3. Cameron, A. G. W. & Benz, W. The origin of the moon and the single impact hypothesis IV. *Icarus* **92**, 204–216 (1991).
4. Cameron, A. G. W. The origin of the Moon and the single impact hypothesis V. *Icarus* **126**, 126–137 (1997).
5. Canup, R. M. & Asphaug, E. Origin of the Moon in a giant impact near the end of the Earth's formation. *Nature* **412**, 708–712 (2001).
6. Benz, W., Slattery, W. L. & Cameron, A. G. W. The origin of the moon and the single-impact hypothesis I. *Icarus* **66**, 515–535 (1986).
7. Benz, W., Slattery, W. L. & Cameron, A. G. W. The origin of the moon and the single-impact hypothesis, II. *Icarus* **71**, 30–45 (1987).
8. Benz, W., Cameron, A. G. W. & Melosh, H. J. The origin of the moon and the single-impact hypothesis III. *Icarus* **81**, 113–131 (1989).
9. Melosh, H. J. & Kipp, M. E. Giant impact theory of the Moon's origin: first 3-D hydrocode results. *Abstr. Lunar Planet. Sci. Conf.* **20**, 685 (1989).
10. Dauphas, N. et al. Magma redox and structural controls on iron isotope variations in Earth's mantle and crust. *Earth Planet. Sci. Lett.* **398**, 127–140 (2014).
11. Melosh, H. J. New approaches to the Moon's isotopic crisis. *Philos. Trans. R. Soc. A* **372**, 20130168 (2014).
12. Stevenson, D. J. & Halliday, A. N. The origin of the Moon. *Philos. Trans. R. Soc. A* **372**, 2014028 (2014).
13. Hauri, E. H., Saal, A. E., Rutherford, M. J. & Van Orman, J. A. Water in the Moon's interior: truth and consequences. *Earth Planet. Sci. Lett.* **409**, 252–264 (2015).
14. Wiechert, U. et al. Oxygen isotopes and the Moon-forming giant impact. *Science* **294**, 345–348 (2001).
15. Spicuzza, M. J., Day, J. M. D., Taylor, L. A. & Valley, J. W. Oxygen isotope constraints on the origin and differentiation of the Moon. *Earth Planet. Sci. Lett.* **253**, 254–265 (2007).
16. Hallis, L. J. et al. The oxygen isotope composition, petrology and geochemistry of mare basalts: evidence for large-scale compositional variation in the lunar mantle. *Geochim. Cosmochim. Acta* **74**, 6885–6899 (2010).
17. Young, E. D. et al. Oxygen isotopic evidence for vigorous mixing during the Moon-forming giant impact. *Science* **351**, 493–496 (2016).

18. Mastrobuono-Battisti, A., Perets, H. B. & Raymond, S. N. A primordial origin for the compositional similarity between the Earth and the Moon. *Nature* **520**, 212–215 (2015).
19. Pahlevan, K. & Stevenson, D. J. Equilibration in the aftermath of the lunar-forming giant impact. *Earth Planet. Sci. Lett.* **262**, 438–449 (2007).
20. Lock, S. J. et al. The origin of the Moon within a terrestrial synestia. *J. Geophys. Res. Planets* **123**, 910–951 (2018).
21. Wang, K. & Jacobsen, S. B. Potassium isotopic evidence for a high-energy giant impact origin of the Moon. *Nature* **538**, 487–490 (2016).
22. Canup, R. M. Forming a Moon with an earth-like composition via a giant impact. *Science* **338**, 1052–1055 (2012).
23. Ćuk, M. & Stewart, S. T. Making the Moon from a fast-spinning Earth: a giant impact followed by resonant despinning. *Science* **338**, 1047–1052 (2012).
24. Reufer, A., Meier, M. M. M., Benz, W. & Wieler, R. A hit-and-run giant impact scenario. *Icarus* **221**, 296–299 (2012).
25. Herwartz, D., Pack, A., Friedrichs, B. & Bischoff, A. Identification of the giant impactor Theia in lunar rocks. *Science* **344**, 1146–1150 (2014).
26. Greenwood, R. C. et al. Oxygen isotopic evidence for accretion of Earth's water before a high-energy Moon-forming giant impact. *Sci. Adv.* **4**, eaao5928 (2018).
27. Sharp, Z. D. A laser-based microanalytical method for the in-situ determination of oxygen isotope ratios of silicates and oxides. *Geochim. Cosmochim. Acta* **54**, 1353–1357 (1990).
28. Shearer, C. K. & Papike, J. J. Basaltic magmatism on the Moon: a perspective from volcanic picritic glass beads. *Geochim. Cosmochim. Acta* **57**, 4785–4812 (1993).
29. Shearer, C. K., Papike, J. J. & Layne, G. D. Deciphering basaltic magmatism on the Moon from the compositional variations in the Apollo 15 very low-Ti picritic magmas. *Geochim. Cosmochim. Acta* **60**, 509–528 (1996).
30. Delano, J. W. Pristine lunar glasses: criteria, data, and implications. *J. Geophys. Res. Solid Earth* **91**, 201–213 (1986).
31. Canup, R. M. Dynamics of lunar formation. *Annu. Rev. Astron. Astrophys.* **42**, 441–475 (2004).
32. Chakraborty, S., Yanchulova, P. & Thiemens, M. H. Mass-independent oxygen isotopic partitioning during gas-phase SiO_2 formation. *Science* **342**, 463–466 (2013).
33. Spera, F. J. Lunar magma transport phenomena. *Geochim. Cosmochim. Acta* **56**, 2253–2265 (1992).
34. Taylor, S. R. & Jakes, P. The geochemical evolution of the moon. In *Proc. 5th Lunar Science Conference* 1287–1305 (Pergamon, 1974).
35. Elardo, S. M., Draper, D. S. & Shearer, C. K. Lunar magma ocean crystallization revisited: bulk composition, early cumulate mineralogy, and the source regions of the highlands Mg-suite. *Geochim. Cosmochim. Acta* **75**, 3024–3045 (2011).
36. Shearer, C. K. et al. Thermal and magmatic evolution of the Moon. *Rev. Mineral. Geochem.* **60**, 365–518 (2006).
37. Ringwood, A. E. & Kesson, S. E. A dynamic model for mare basalt petrogenesis. In *Proc. 7th Lunar and Planetary Science Conference* 1697–1722 (Pergamon, 1976).
38. Kesson, S. E. & Ringwood, A. E. Mare basalt petrogenesis in a dynamic moon. *Earth Planet. Sci. Lett.* **30**, 155–163 (1976).
39. Hess, P. C. & Parmentier, E. M. A model for the thermal and chemical evolution of the Moon's interior: implications for the onset of mare volcanism. *Earth Planet. Sci. Lett.* **134**, 501–514 (1995).
40. Zhong, S., Parmentier, E. M. & Zuber, M. T. A dynamic origin for the global asymmetry of lunar mare basalts. *Earth Planet. Sci. Lett.* **177**, 131–140 (2000).
41. Cao, X. et al. Triple oxygen isotope constraints on the origin of ocean island basalts. *Acta Geochim.* **38**, 327–334 (2019).
42. Pack, A. & Herwartz, D. The triple oxygen isotope composition of the Earth mantle and understanding variations in terrestrial rocks and minerals. *Earth Planet. Sci. Lett.* **390**, 138–145 (2014).
43. Meyer, C. *Lunar Sample Compendium* (NASA/ARES, 2012);https://go.nature.com/39TEW6O

Methods

Laser fluorination oxygen isotope analysis. Oxygen isotope analyses were made at the Center for Stable Isotopes, University of New Mexico, using the standard laser fluorination technique[27] with a modified O_2 purification process to obtain ultra-high-precision results for $\Delta'^{17}O$. For whole-rock analysis, sample chips were selected that were as homogeneous as possible and representative of the larger sample's overall composition. Fragments of samples were used as opposed to powders to minimize the amount of possible adsorbed water on the surface. Samples for mineral separate analysis were crushed and sieved, and grains were separated using standard magnetic, heavy liquid and finally hand-picking techniques. About 2 mg of sample material along with equal-sized in-house standards were loaded into a 44-well nickel sample plate. A San Carlos olivine laboratory standard was run multiple times in each daily session. The San Carlos olivine is calibrated to Vienna Standard Mean Ocean Water (VSMOW) and Standard Light Antarctic Precipitation (SLAP) values from Wostbrock et al.[44], where both VSMOW2 and SLAP2 were fluorinated to release O_2, allowing for a direct determination of the $\delta^{17}O$ and $\delta^{18}O$ values of our olivine standard in relation to the international water standards. The $\delta^{18}O_{VSMOW2} - \delta^{18}O_{SLAP2}$ value was −55.55‰ and $\Delta'^{17}O_{VSMOW2} - \Delta'^{17}O_{SLAP2} = -0.015‰$ (ref. [44]), demonstrating that no stretching factor is required (for example, ref. [45]). Replicate analyses of the San Carlos olivine give the following values: ($\delta'^{17}O = 2.716‰$ and $\delta'^{18}O = 5.255‰$, relative to VSMOW2–SLAP2. The $\Delta'^{17}O$ value of our laboratory San Carlos standard is $-0.058 \pm 0.004‰$, based on $\lambda = 0.528$ (see Supplementary Table 1). All oxygen isotope measurements herein are calibrated to this San Carlos olivine laboratory standard.

The sample plate was loaded into the fluorination chamber and evacuated using a turbomolecular pump for 24–48 h before sample analysis, being heated with an external heat lamp during the entire pump-down period. BrF_5 gas was used to prefluorinate the samples before analysis, allowing any remaining surface contamination or H_2O to react and be removed. This was done by introducing 120 mbar of BrF_5 to the sample chamber and allowing it to react for 1 h at room temperature. Any byproducts produced by this prefluorination reaction were removed through the waste portion of the oxygen fluorination line.

Samples were heated with a CO_2 laser in the presence of 100 mbar of BrF_5. The O_2 gas that was generated from the fluorination of the sample and excess BrF_x compounds were passed over a series of cryogenic traps to remove BrF_x and finally heated NaCl to remove any traces of F_2. The oxygen was adsorbed on a 5 Å molecular sieve trap submerged in liquid nitrogen. After collection of the oxygen, the molecular sieve trap was heated, releasing the oxygen into a stream of helium carrier gas that passes through a 6 ft × 1/8" (1.83 m × 3.2 mm) 60/80 Mol Sieve 13X gas chromatograph (GC) column. The GC quantitatively separates O_2 from traces of NF_3, which has a mass interference at mass 33 ($^{16}O^{17}O$)[17,25]. It is our experience that the chromatographic separation is the best way to ensure high-purity O_2.

The $\delta^{17}O$ and $\delta^{18}O$ values of the sample gas were measured on a Thermo Fisher MAT 253 Isotope Ratio Mass Spectrometer using a reference gas calibrated to VSMOW and SLAP. Each sample run consisted of 40 iterations, in which each iteration included a 26 s collection time for the reference and sample gas separated by a 15 s delay. These long collection times allow us to obtain reproducible, high-precision $\Delta'^{17}O$ values.

Triple oxygen isotope systematics and choice of λ. $\delta^{17}O$ and $\delta^{18}O$ values are defined as:

$$\delta^x O = \left(\frac{R_{sample}}{R_{standard}} - 1\right) \times 1{,}000 \quad (1)$$

where R is the $^{18}O/^{16}O$ or $^{17}O/^{16}O$ ratio, depending on x. All plots in this paper use a linearized form of delta notation[46], which is denoted by δ' where:

$$\delta' = 1{,}000 \ln\left(\frac{\delta}{1{,}000} + 1\right) \quad (2)$$

For the triple oxygen isotope system, mass-dependent fractionation between two phases A and B in thermodynamic equilibrium is given by the equation[42,44,47]:

$$\alpha^{17}O_{A-B} = \left(\alpha^{18}O_{A-B}\right)^{\theta} \quad (3)$$

or

$$\ln \alpha^{17}O_{A-B} = \theta\left(\ln \alpha^{18}O_{A-B}\right) \quad (4)$$

where θ is the triple isotope fractionation exponent, which can be further defined in linearized form by the equation:

$$\theta_{A-B} = \frac{\delta'^{17}O_A - \delta'^{17}O_B}{\delta'^{18}O_A - \delta'^{18}O_B} \quad (5)$$

The terrestrial fractionation line (TFL) is the best-fit line in $\delta'^{17}O$–$\delta'^{18}O$ space for terrestrial samples not affected by photochemical effects[48]. The general equation for the linearized form of the TFL is given as:

$$\delta'^{17}O = \lambda \times \delta'^{18}O + \gamma \quad (6)$$

where λ is defined as the empirically derived slope of the best-fit line for this data and γ is the y intercept[44]. The γ term is normally taken as zero. Small departures from the TFL, which are the main focus of this paper, are best illustrated using the $\Delta'^{17}O$ notation where:

$$\Delta'^{17}O = \delta'^{17}O_{measured} - \lambda \times \delta'^{18}O \quad (7)$$

Different publications have chosen to use different λ reference values for their presentation of $\Delta'^{17}O$ values. For example, Pack and Herwartz[42] use a value of 0.5305 because it is the theoretical high temperature limit for λ[47,49]. Starkey et al.[50] use a value of 0.5247, which is based on the best fit of 47 terrestrial whole-rock and mineral separate samples. In this study, we use a value of 0.528, which approximates most natural data[51] and is adopted exclusively by the meteorological community as a best fit to the global meteoric water line. We stress that the choice of a λ value is arbitrary and does not change any of the interpretations or conclusions obtained in any triple isotope publication. All of the conclusions in this paper would remain unchanged if we chose a different reference λ value.

Standardization. The triple oxygen isotope community has yet to reach a consensus on a standard reference line for defining $\Delta'^{17}O$ values. The three most recent papers on lunar oxygen use three different methods for reporting their $\Delta'^{17}O$ data. Herwartz et al.[25] choose to report their $\Delta'^{17}O$ values relative to the international standard VSMOW, as done in this paper. Young et al.[17] define their $\Delta'^{17}O$ values relative to San Carlos olivine with a $\Delta'^{17}O$ of −0.1‰ (VSMOW reference $\lambda = 0.5305$), and Greenwood et al.[26] choose to use a value of −0.064‰ (VSMOW, reference $\lambda = 0.5262$). We suggest that rock $\delta^{17}O$, $\delta^{18}O$ and $\Delta'^{17}O$ data should be reported relative to the VSMOW scale established by the IAEA to ensure that data from both the hydrological and solid earth communities remain comparable.

Young et al.[17] report their data relative to San Carlos olivine rather than VSMOW. This was done to eliminate uncertainties in calibration of silicates to the VSMOW–SLAP scale and makes sense if the silicates are not well calibrated to the VSMOW–SLAP scale. Notably, it has been shown that some San Carlos olivine is heterogeneous[50], making it a poor choice on which to define a silicate reporting scale that would be used by multiple laboratories. The argument against using the established water standard typically relies on the fact that rocks and water are typically measured using different analytical procedures, since the direct fluorination of water is challenging. However, our San Carlos olivine laboratory standard is homogeneous and was calibrated to VSMOW and SLAP fluorinated utilizing the same extraction lines and mass spectrometer in our laboratory[44]. This allows for a direct determination of the $\delta^{17}O$ and $\delta^{18}O$ values of our olivine standard in relation to the international water standards. Given our clear reporting scheme, it is possible for anyone to convert our data to any other reference scale that might be adopted in the future.

Data availability

The authors declare that the necessary data supporting the findings of this study are available within the paper and its supplementary information files. All other datasets generated during and/or analysed during the current study are available from the corresponding author on reasonable request.

References

44. Wostbrock, J. A. G., Cano, E. J. & Sharp, Z. D. An internally consistent triple oxygen isotope calibration of standards for silicates, carbonates and air relative to VSMOW2 and SLAP2. *Chem. Geol.* **533**, 119432 (2020).
45. Pack, A. et al. The oxygen isotope composition of San Carlos olivine on the VSMOW2–SLAP2 scale. *Rapid Commun. Mass Spectrom.* **30**, 1495–1504 (2016).
46. Miller, M. F. Isotopic fractionation and the quantification of 17O anomalies in the oxygen three-isotope system: an appraisal and geochemical significance. *Geochim. Cosmochim. Acta* **66**, 1881–1889 (2002).
47. Young, E. D., Galy, A. & Nagahara, H. Kinetic and equilibrium mass-dependent isotope fractionation laws in nature and their geochemical and cosmochemical significance. *Geochim. Cosmochim. Acta* **66**, 1095–1104 (2002).
48. Thiemens, M. H. Mass-independent isotope effects in planetary atmospheres and the early solar system. *Science* **283**, 341–345 (1999).
49. Cao, X. & Liu, Y. Equilibrium mass-dependent fractionation relationships for triple oxygen isotopes. *Geochim. Cosmochim. Acta* **75**, 7435–7445 (2011).
50. Starkey, N. A. et al. Triple oxygen isotopic composition of the high-3He/4He mantle. *Geochim. Cosmochim. Acta* **176**, 227–238 (2016).

51. Sharp, Z. D., Wostbrock, J. A. G. & Pack, A. Mass-dependent triple oxygen isotope variations in terrestrial materials. *Geochem. Perspect. Lett.* **7**, 27–31 (2018).
52. Chiba, H., Chacko, T., Clayton, R. N. & Goldsmith, J. R. Oxygen isotope fractionations involving diopside, forsterite, magnetite, and calcite: application to geothermometry. *Geochim. Cosmochim. Acta* **53**, 2985–2995 (1989).

Acknowledgements

We are grateful to NASA and CAPTEM for approving our requests for Apollo samples used in this study. We thank F. Trusdell, M. Perfit, V. S. Kamenetsky, L. S. Crumpler, K. A. Smart, S. Tappe, S. C. Kruckenberg, B. Oller, G. Wörner, L. D. Ashwal and L. E. Borg for the collection and/or donation of sample material. Thank you to S. Locke for sharing his thoughts on post-giant impact dynamics. Thank you to S. Chakraborty and M. H. Thiemens for sharing additional insight regarding their work on mass-independent oxygen isotope fractionation in gas-phase SiO_2 formation. We acknowledge support from NSF award 1903852.

Author contributions

Analyses were made by E.J.C., who also wrote the initial manuscript. All authors contributed ideas, helped construct the project and contributed additions and edits to the initial manuscript.

Competing interests

The authors declare no competing interests.

Additional information

Extended data is available for this paper at https://doi.org/10.1038/s41561-020-0550-0.

Supplementary information is available for this paper at https://doi.org/10.1038/s41561-020-0550-0.

Correspondence and requests for materials should be addressed to E.J.C.

Peer review information Primary Handling Editor: Tamara Goldin.

Reprints and permissions information is available at www.nature.com/reprints.

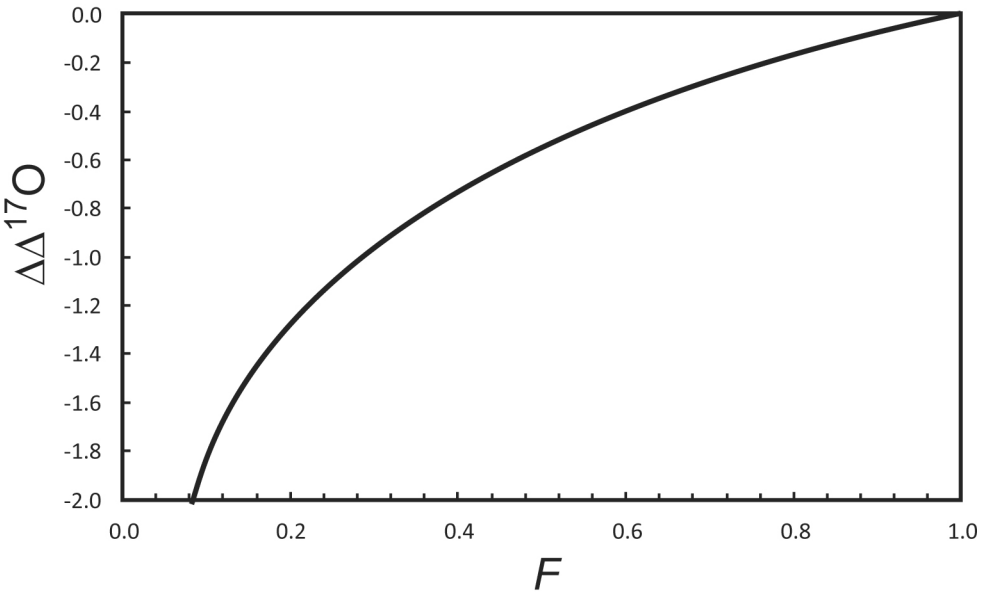

Extended Data Fig. 1 | Plot of the change in the Δ′^{17}O value (ΔΔ′^{17}O) of the lunar vapour as a function of the amount lost during early deposition and incorporation into the bulk Moon (*F*). If 60% of the vapour is removed into the mantle (*F*=0.4), the remaining vapour will have a Δ′^{17}O value that is 0.75‰ lighter than the initial vapour (bulk Moon value). In order to change the outer 50 km of the 'crust' by 0.05‰, ~4×10^{23} g of vapour would have to be remixed into the outer crust. The effect on the δ^{18}O value would be minimal.

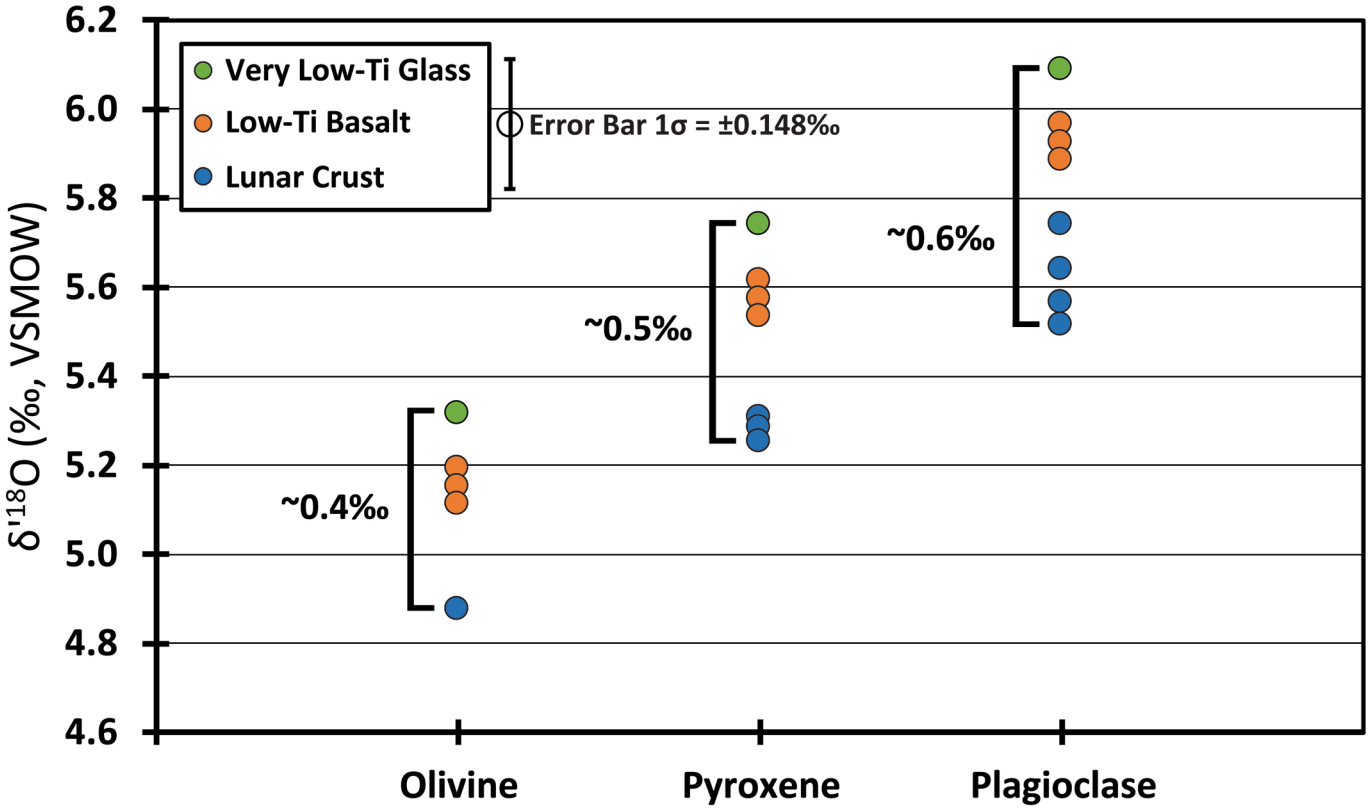

Extended Data Fig. 2 | Plot of $\delta'^{18}O$ values of mineral separates from selected lunar samples. Mineral separate data from the lunar crust samples are measured values and include plagioclase, pyroxene and/or olivine separates from samples 60016, 62237, 77215, and 78238. Mineral separate data for low-Ti Basalts (samples 12018, 12063, 15016, and 15426) are calculated from the whole-rock $\delta'^{18}O$ measurements using simple mass-balance equations, modal mineral percentages, and expected isotope fractionations. The 'theoretical' mineral values for the VLT glass are calculated from modes estimated from the CIPW norm for this sample. Calculated $\delta^{18}O$ mineral separate data, either from CIPW norm or measured modes agree to within <0.1‰. Mineral modes and bulk composition data used to calculate the CIPW norm values are from the Lunar Sample Compendium[43]. The isotope fractionations used in the mass balance equations are $\Delta'^{18}O_{Pl\text{-}Ol} = 0.774$, $\Delta'^{18}O_{Pl\text{-}Px} = 0.35$, $\Delta'^{18}O_{Px\text{-}Ol} = 0.424$ (from Chiba et al.[52]) and assume isotopic equilibrium between mineral phases at 1200 °C.

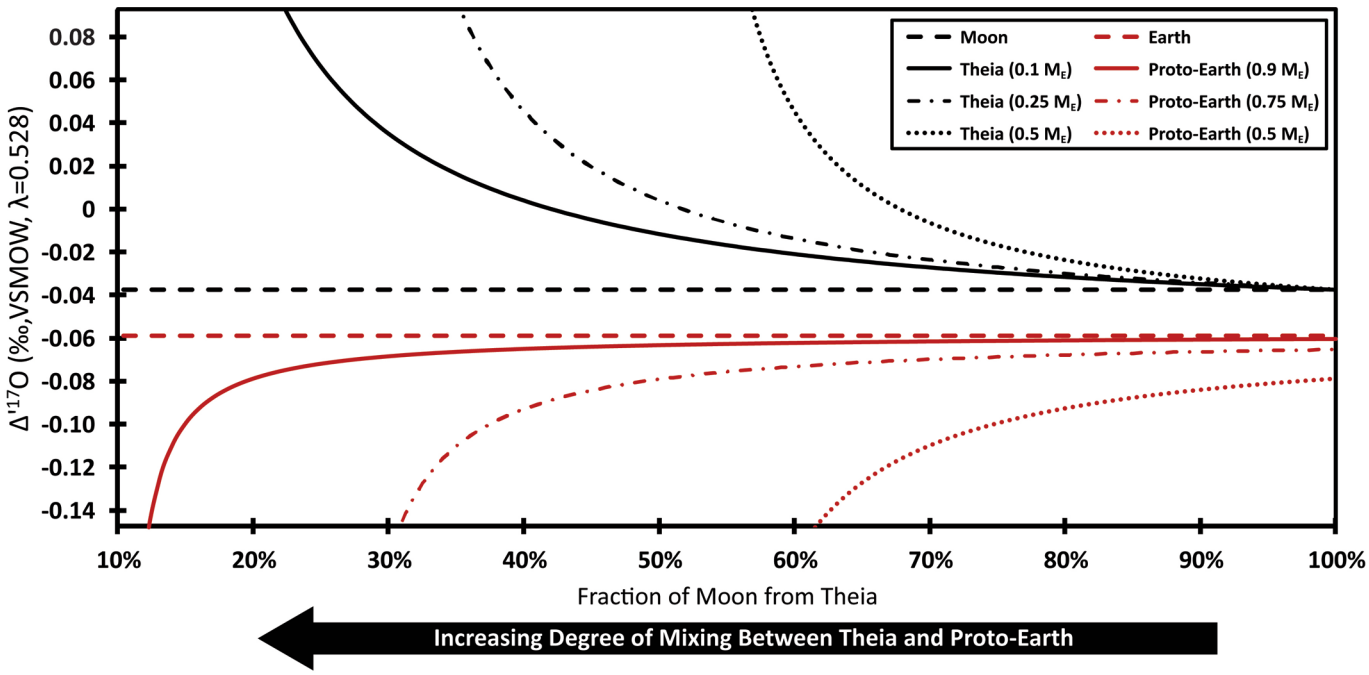

Extended Data Fig. 3 | Calculated Δ′^{17}O values for Theia and Proto-Earth for varying degrees of mixing and initial proto-planet masses. The plot illustrates the calculated Δ′^{17}O values for Theia and Proto-Earth given varying initial Theia masses (indicated by different line styles) and the percentage of the Moon that is composed of material from Theia. For example, if Theia was initially 0.1 M_E and 70% of the Moon is material from Theia, Theia's initial Δ′^{17}O value was about −0.028‰ and Proto-Earth's was about −0.062‰. This assumes that the current values of the Moon and Earth are −0.038‰ and −0.060‰ respectively and the summed masses of Theia and Proto-Earth are equivalent to the total mass of the present Earth-Moon system. Increased mixing between Theia and Proto-Earth produce smaller amounts of Theia in the Moon.

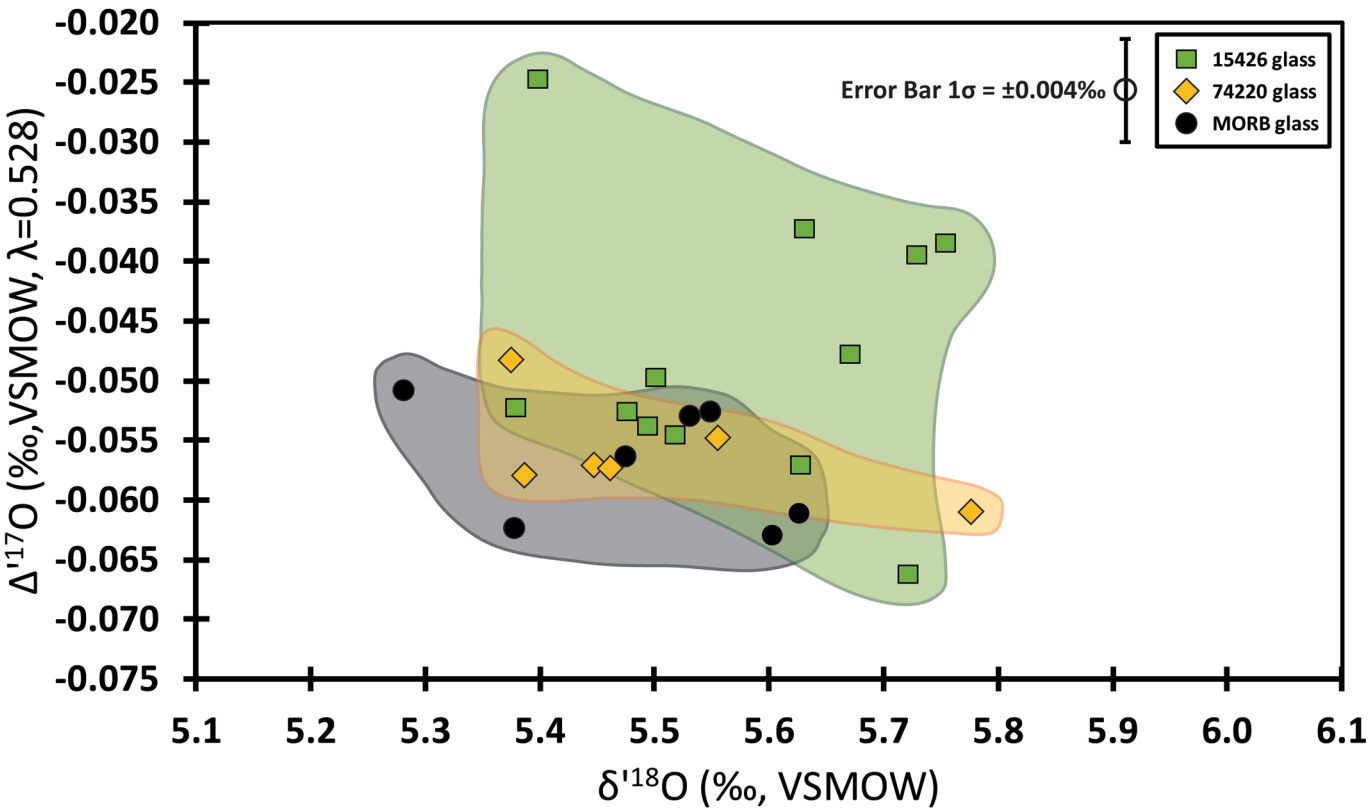

Extended Data Fig. 4 | Plot of Plot of $\Delta'^{17}O$ versus $\delta'^{18}O$ for the VLT green glass (15426), high-Ti orange/black glass (74220), and MORB glass (ALV2746-12). The VLT green glass is represented by the green squares and high-Ti orange/black glass is represented by the yellow diamonds. The MORB glass values are black circles. The coloured in shapes highlight the range in oxygen isotope values for their corresponding data set. This illustrates how large the range seen in the VLT green glass is compared to that seen in homogeneous glass samples measured with identical methods. The green glass has a range over three times that of the high-Ti orange/black glass and the MORB sample, demonstrating that the isotopic heterogeneity in the green glass beads is not a product of the sample analysis and is real variation.

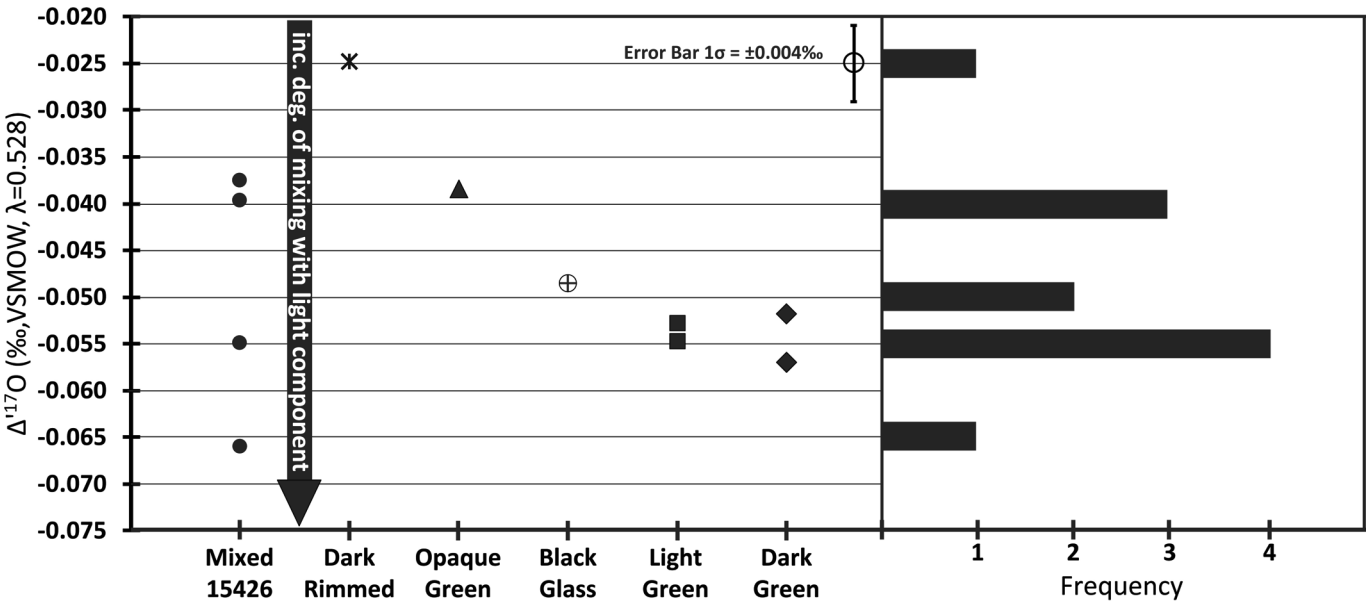

Extended Data Fig. 5 | Plot of $\Delta'^{17}O$ values for different fractions of very low-Ti green glass (left) with histogram (right). Various fractions of VLT green glass (sample 15426) were separated by glass bead appearance and measured. Mixed fractions of the green glass containing a random assortment of glass beads ranged from −0.066‰ to −0.037‰, a spread far greater than what can be attributed to analytical error on measurements of a homogeneous sample. When separated by visual appearance, samples ranged from −0.057‰ to −0.025‰ with the dark rimmed fraction having the heaviest measured $\Delta'^{17}O$ value in this study. Histogram bins are 0.005‰ wide and include both mixed and separated fractions combined to illustrate the frequency distribution of the measured values.